Article

Not peer-reviewed version

# SARS-CoV-2 Entry Can Be Mimicked in *C. elegans* Expressing Human ACE2: A New Tool for Pharmacological Studies

Margherita Romeo , Sara Baroni , Maria Monica Barzago , Samuela Gambini , Ada De Luigi , Daniela Iaconis , Andrea Rosario Beccari , Maddalena Fratelli , Luisa Diomede *

Posted Date: 18 September 2025

doi: 10.20944/preprints202509.1598.v1

Keywords: COVID-19; SARS-CoV-2; receptor binding domain; angiotensin-converting enzyme 2; *C. elegans*; pseudo infection; raloxifene

*Article*

# SARS-CoV-2 Entry Can Be Mimicked in *C. elegans* Expressing Human ACE2: A New Tool for Pharmacological Studies

**Margherita Romeo [1,†], Sara Baroni [1,†], Maria Monica Barzago [1], Samuela Gambini [1], Ada De Luigi [1], Daniela Iaconis [2], Andrea Rosario Beccari [2], Maddalena Fratelli [1] and Luisa Diomede [1,*]**

[1] Department of Molecular Biochemistry and Pharmacology, Istituto di Ricerche Farmacologiche Mario Negri IRCCS, Milano, Italy

[2] EXSCALATE, Dompé Farmaceutici SpA, Via Tommaso De Amicis, 95, 80131, Napoli, Italy

* Correspondence: luisa.diomede@marionegri.it

† These authors equally contributed to the work.

**Abstract**

Testing medical countermeasures for SARS-CoV-2 transmission using vertebrates can be slowed by legislation regulating animal experimentation, high costs, and ethical concerns. To overcome these challenges, we propose a new *Caenorhabditis elegans* strain that constitutively expresses the human angiotensin-converting enzyme 2 receptor (ACE2). This resulted in significant impairment of reproduction and a defect in pharyngeal function compared to wild-type (WT) worms. SARS-CoV-2 infection was simulated by treating worms with the receptor-binding domain (RBD) of the virus, which caused dose- and time-dependent pharyngeal impairment in ACE2 worms but not in WT worms. The toxicity of RBD was prevented by administering an anti-human ACE2 antibody, demonstrating that interaction with the ACE2 receptor is essential. The ACE2-expressing worm strain was further used for pharmacological research with Raloxifene. In vitro, Raloxifene at 1-3 μM reduced the entry of lentiviral particles carrying the Wuhan variant, B.1.1.7 UK, and B.1.1.529 Omicron strains, into HEK293-ACE2, as well as particles expressing N501Y- or P681H-mutated spike proteins. Raloxifene (0.1-1 μM) completely counteracted RBD toxicity in ACE2 worms, indicating that this strain offers a cost-effective in vivo screening platform for molecules whose effects involve interaction with the ACE2 receptor.

**Keywords:** COVID-19; SARS-CoV-2; receptor binding domain; angiotensin-converting enzyme 2; *C. elegans;* pseudo infection; raloxifene

## 1. Introduction

The negative pandemic experience of Coronavirus Disease 2019 (COVID-19), with over 7 million deaths and 778 million infected people worldwide [1], has taught us how the emergence of a new infectious agent in a globalized society causes devastating effects and how crucial it is to be prepared for new infections. At the same time, important lessons were learned about detecting and isolating the emerging pathogen, quickly understanding its effects, and testing candidate prophylactic and therapeutic strategies. Significant efforts were dedicated to studying the transmission, pathogenesis, and medical countermeasures of SARS-CoV-2. For this purpose, different vertebrate animals were used, including mice, non-human primates, hamsters, and ferrets [2]. However, we experienced how pharmacological studies were slowed down by strict national and international laws regulating animal experimentation, especially in infection studies requiring high biosafety levels, and by the high costs associated with using vertebrate animals. To overcome these limitations, having a cost-effective and more practical model could be very helpful.

 doi:10.20944/preprints202509.1598.v1



In this context, the invertebrate *Caenorhabditis (C.) elegans* offers several advantages, such as easy cultivation in the laboratory, low maintenance costs, and a short lifespan. These features make it a valuable model for in vivo preclinical pharmacological screening before testing drug candidates in vertebrate studies. This nematode has recently been used to study some bacterial and viral infections [3]. It has developed several responses to pathogens to survive and reproduce, but unlike higher eukaryotes, it does not show adaptive immunity. The response is often triggered within the cells by detecting infection-induced damage, mainly in the intestine or epidermis [4]. When encountering pathogenic microorganisms, *C. elegans* activates protective mechanisms, including an avoidance behavior, by detecting specific microbial molecules [5]. When a pathogen cannot be avoided, the nematode can mount an innate immune response by activating specific signaling pathways, producing and releasing defense molecules [6].

This study aimed to characterize a new transgenic *C. elegans* strain constitutively expressing the human angiotensin-converting enzyme 2 (hACE2) receptor. Although *C. elegans* has an ortholog of the human ACE2 gene called *acn-1*, which encodes for an ACE-like protein with metallopeptidase activity, this protein has functions unrelated to human ACE2. ACN-1 protein is required for larval development and adult morphogenesis and is hypothesized to be involved in larval seam cell fusion [7–9]. To mimic the infection and investigate the use of this model for quick and cheap pre-clinical studies, ACE2-expressing worms were administered with the Receptor-Binding Domain (RBD) of SARS-CoV-2. This was based on the knowledge that one of the main routes of infection in *C. elegans* occurs upon ingestion through the pharynx and establishing an intestinal colonization [10]. The onset of a specific RBD-induced toxic effect was assessed by scoring the worms' pharyngeal motility and locomotion. This is because *C. elegans* can recognize human proteins with biologically relevant properties by developing specific dysfunctions in the pharynx or neuromuscular system [11].

To investigate the possible use of this model for pharmacological approaches as a prototype drug, we employed Raloxifene, a compound proposed as an effective and safe anti-COVID-19 treatment. Although it belongs to the second-generation selective estrogen receptor modulator clinically used for treating and preventing post-menopausal osteoporosis and cancer, Raloxifene exerts an antiviral activity against pathogens such as influenza A, Ebola, and hepatitis C [12]. In addition, from the screening of compound libraries conducted by the Exscalate4CoV consortium within the European Commission's Horizon 2020 program on 400,000 candidates, Raloxifene resulted as the most promising drug based on its ability to regulate SARS-CoV-2 replication and reduce the pro-inflammatory cytokines [13,14]. Data obtained from a small randomized controlled multicentre clinical trial in patients with mild to moderate symptoms suggested a possible capability of the drug to reduce the viral load, limiting the diffusiveness and contagiousness in the population, being the proportion of participants with undetectable SARS-CoV-2 greater in subjects treated for seven days with 60 or 120 mg/day Raloxifene compared to the placebo group [14]. In vitro experiments on Vero E6 and Calu-3 cells showed that Raloxifene exerts an antiviral activity blocking SARS-CoV-2 replication [15]. Moreover, surface plasmon resonance studies from our group have recently reported that this compound can directly bind, although with low affinity, to the Spike protein of SARS-CoV-2, its subunit 1, and the RBD [15]. However, it cannot be excluded that Raloxifene can directly influence viral entry machinery in other experimental conditions, possibly modulating host response.

Before testing the effect of Raloxifene in transgenic *C. elegans*, in vitro studies were conducted in human embryonic kidney 293-T cells stably expressing hACE2 (HEK293-ACE2) pseudo-infected with lentiviral vectors expressing different Spike variants on the envelope. Overall, the results obtained indicate that the new transgenic *C. elegans* strain expressing the human ACE2 represents a good experimental approach for modeling the SARS-CoV-2 infection and that Raloxifene can affect the interaction between SARS-CoV-2 and ACE2, inhibiting viral entry.

## 2. Materials and Methods

*C. elegans*

 doi:10.20944/preprints202509.1598.v1



Bristol N2 nematodes were obtained from the Caenorhabditis Genetics Center (CGC, Minnesota, USA) and labeled as wild-type (WT). The transgenic *C. elegans* strain expressing the hACE2 sequence fused with an mCherry reporter gene at the C-terminus, under the control of the Vacuolar H ATPase (vha)-6 promoter (*vha6*::ACE2::mCherry), was acquired from InVivo Biosystems (Eugene, USA) and designated as ACE2. All *C. elegans* strains were cultured and maintained using standard breeding conditions. Experiments were conducted at 20°C on standard Nematode Growth Media (NGM) seeded with *Escherichia coli (E. coli)* OP50 as food (CGC).

*Brood size and Larval Development*

The impact of ACE2 expression on reproduction and larval development was determined in WT and ACE2-synchronized worms by singly plating them at the L4 larval stage on NGM-agar plates seeded with *E. coli* OP50. Starting the following day, the number of eggs laid by each worm was recorded daily until egg-laying ceased. Larval development, under the same experimental conditions, was monitored daily, and the number of individuals at each larval stage was scored until they reached the adult stage.

*Pharyngeal Behavior and Motility*

To evaluate the effect of hACE2 expression, the pharyngeal function and motility were assessed in synchronized WT and ACE2 worms at their 1-day adulthood. Only worms crawling on the bacteria were considered for the assays. The pharyngeal function was measured by counting the number of times the terminal bulb of the pharynx contracted in 1 minute (pumps/min) [16]. To measure worms' motility, worms were picked up and transferred into a well of a 96-well plate containing 100 µL of 10 mM phosphate-buffered saline (PBS), pH 7.4. The body bend assay was scored by counting the number of left-right movements in 1 minute (body bends/min).

To evaluate the worms' sensitivity to chemical stressors, WT and ACE2 nematodes were exposed to $H_2O_2$. Briefly, L4 larvae were collected, washed with M9 buffer to eliminate bacteria, and then exposed to 0.5 mM $H_2O_2$ in 10 mM PBS, pH 7.4, for 2 hours (100 worms/100 µL) or to the same volume of 10 mM PBS, pH 7.4, alone (vehicle) as a control. The worms were plated onto NGM plates seeded with *E. coli* OP50, and the pharyngeal pumping was scored 24 hours later.

*Lifespan and Health Span*

The lifespan and health span of WT and ACE2 worms were evaluated at 20°C, maintaining nematodes on standard NGM seeded with *E. coli* OP50. The nematodes were synchronized by egg-laying and transferred to fresh NGM plates daily during the fertile period to avoid overlapping generations. Dead, alive, and censored animals were scored during the transferring process. The animals were counted as dead when they had neither moved nor reacted to a manual stimulus with a platinum wire, nor had any pharyngeal pumping activity. Animals with exploded vulvas or those desiccated on the wall were censored [17]. The number of active movements was also assessed in nematodes employed for the lifespan assay to determine their healthy aging. Animals crawling spontaneously or after a manual stimulus were considered moving, while dead animals and animals without crawling behavior were considered not moving.

*Exposure of C. elegans to RBD*

To mimic the infection with SARS-CoV-2, WT and ACE2 transgenic worms were fed with the RBD of SARS-CoV-2 in the Wuhan variant. Nematodes were synchronized by egg-laying, and 48 hours later, L4 larvae were collected from the plates and washed thrice with 10 mM PBS, pH 7.4, to remove bacteria. Worms were incubated with 0.00001-1000 ng/mL SARS-CoV-2 RBD (Trenzyme, Konstanz, Germany) (100 worms/ 100µL) for 2 hours at 20°C on an orbital shaker and then plated on NMG plates seeded with *E. coli* OP50. Control worms were incubated with only 10 mM PBS, pH 7.4 (vehicle). The pharyngeal pumping rate and the body bends were scored 2 and 24 hours later.

 doi:10.20944/preprints202509.1598.v1



To determine if the toxic effect of the RBD administration was explicitly due to the binding of RBD to the hACE2 receptors expressed in the transgenic nematodes, the anti-human ACE2 antibody (anti-hACE2, Santa Cruz Biotechnology, USA) was diluted at 1:200 (vol/vol) in 10 mM PBS, pH 7.4, and incubated for 1 hour at room temperature with 100 ng/mL RBD before the administration to the worms (100 worms/100 µL). In addition, the anti-hACE2, diluted as previously described, was inactivated at 100°C for 15 minutes and incubated with 100 ng/mL RBD for 1 hour at room temperature before the administration to the worms (100 worms/100 µL). Control worms were fed with the anti-hACE2 antibody diluted at 1:200 (vol/vol) in 10 mM PBS, pH 7.4, or 10 mM PBS, pH 7.4 only (vehicle). After a 2-hour incubation with orbital shaking, worms were transferred onto NGM plates seeded with *E. coli* OP50, and the pharyngeal motility was assessed 2 and 24 hours later.

*Cells*

HEK293 and HEK293-ACE2 [18] were maintained in Dulbecco Modified Eagle Medium (DMEM; Euroclone S.p.A., Pero, Milan, Italy; cod. ECB7501L) containing 10% heat-inactivated fetal bovine serum (FBS, Gibco, Thermo Fisher, Segrate, Milan, Italy; cod. 10270), L-glutamine (Gibco; cod. 25030-024), non-essential amino acids (Euroclone; cod. ECB3054D), and penicillin/streptomycin (Corning, New York, NY, USA; cod. 20-002-Cl). HEK293-ACE2 required puromycin (Genespin, Milano, Italy). Cells were cultured in T25 flasks at 37°C in a humidified 5% $CO_2$ and routinely split every 4–5 days. Cells used in this study had not been passaged more than 20 times from the original stock.

*Cell Viability*

HEK293-ACE2 cells were seeded (2 x $10^4$ cells/well) on 96-well plates in a complete DMEM medium with 10% FBS. After incubation for 24 hours at 37°C in humidified 5% $CO_2$, the medium was replaced with a fresh one containing Raloxifene (Dompé farmaceutici S.p.A., Milano, Italy) previously dissolved at 10 mM in dimethyl sulfoxide (DMSO) and diluted in DMEM at 1 – 30 µM. Control cells were treated with an equivalent DMSO concentration (Vehicle). Cells were incubated for 24 hours at 37°C in humidified 5% $CO_2$, and the medium was replaced with a fresh one without Raloxifene. After an additional incubation of 24 hours at 37°C in humidified 5% $CO_2$, HEK293-ACE2 cells were treated with 5 mg/mL 3-(4,5-dimethylthiazol-2-yl)-2,5 2,5-diphenyltetrazolium bromide (MTT; Sigma Aldrich, St. Louis, MO, USA) in 10 mM PBS, pH 7.4. After incubation for 4 hours at 37°C, MTT was removed, and the cells were resuspended in isopropanol containing 0.04 M HCl. The absorbance of the samples was determined at 560 nm using a spectrophotometer (Infinite M200, Tecan, Männedorf, Switzerland), and the cell viability was expressed as a percentage of vehicle-treated cells.

*Transduction Assay*

HEK293-ACE2 and HEK293 cells were seeded (2 x $10^4$ cells/well) on 96-well plates in a complete DMEM medium with 10% FBS. To evaluate the effect of Raloxifene on the early stage of the viral infection, after 24 hours at 37°C in humidified 5% $CO_2$, the medium was replaced with fresh medium containing Raloxifene, previously dissolved at 10 mM in DMSO and diluted in DMEM at 1 or 3 µM. Control cells were treated with an equivalent DMSO concentration (Vehicle). Cells were then incubated for 4 hours at 37°C in humidified 5% $CO_2$ and then infected in the presence of 10 µg/mL Polybrene (VectorBuilder, USA) with 5 – 50 MOI lentiviral vectors exposing the SARS-CoV-2 Spike protein as surface glycoprotein in the Wuhan, B.1.1.7 UK, B.1.351 SA, N501Y or P681H variant with eGFP as gene reporter or B.1.1.529 Omicron variant with eRFP as gene reporter (VectorBuilder, USA). HEK293 cells were infected with lentiviral vectors as negative controls. Non-infected and non-drug-treated cells were employed as additional controls. The medium was replaced with a fresh one the day after the transduction. After a further 24 hours of incubation at 37°C in humidified 5% CO2, the transduction efficiency was checked by determining the percentage of cells expressing GFP or RFP

 doi:10.20944/preprints202509.1598.v1



using a ZOETM fluorescent cell imager (Bio-Rad, Hercules, CA, USA). The ZOETM images were analyzed with Fiji software, an open-source platform for biological image analysis [18]. The transduction efficiency was expressed as the percentage of cells positive for GFP- or RFP-fluorescent signal.

*Raloxifene Administration to C. elegans*

Raloxifene was dissolved in DMSO at a concentration of 10 mM, diluted to 0.001-5 µM in 10 mM PBS, pH 7.4, and incubated for 1 hour at room temperature with 100 ng/mL RBD before the administration to WT and ACE2 worms (100 worms/100 µL). Control worms were fed 100 µL Raloxifene or 10 mM PBS, pH 7.4 (Vehicle). The pharyngeal pumping rate, measured by counting the number of times the terminal bulb of the pharynx contracted over a 1-minute interval (pumps/min), was scored 2 and 24 hours later.

*Western Blot Analysis*

HEK293-ACE2 cells, treated for 3, 6, and 24 hours with 3 µM Raloxifene or the corresponding volume of DMSO diluted in DMEM (Vehicle) were lysed for 15 minutes at 4°C with 20 mM Tris-HCl, pH 7.5, containing 150 mM NaCl, 1 mM $Na_2EDTA$, 1 mM EGTA, 1% NP-40, 1% sodium deoxycholate, 2.5 mM sodium pyrophosphate, 1 mM β-glycerophosphate, 1 mM $Na_3VO4$ and 1 µg/mL leupeptin. Samples were centrifuged for 10 minutes at 16,100 x *g*, and the protein content was quantified using a Pierce BCA Protein Assay Kit (Thermo Fisher Scientific Inc., Rockford, USA). Twenty µg of total protein was loaded in each lane.

Protein extracts were also prepared from *C. elegans* using the following protocol. ACE2 and WT nematodes were synchronized by egg-laying and cultured at 20°C on NGM plates seeded with *E. coli* OP50 as food. Worms on the first day of adulthood were collected with M9 buffer and washed to eliminate bacteria. Pellets were resuspended in 300 µL of 10 mM PBS, pH 7.4, and supplemented with protease inhibitor cocktail (Millipore, Milan, Italy). The samples were sonicated at 4°C using the Bioruptor® sonicator device (Diagenode, SA., Ougreé, Belgium) at 30 sec/30 sec on and off intervals for 15 minutes on maximum energy. After centrifuging the samples at 15700 x *g* for 5 minutes at 4°C, the supernatants were transferred to a clean 1.5 mL tube, and the protein concentration was determined using the Bradford Assay (Bio-Rad). Twenty-five µg of total protein was loaded in each lane. In addition, 20 ng of recombinant hACE2 protein (AdipoGen Life Sciences, Fuellinsdorf, Switzerland) was loaded as a control.

Proteins were separated by 10% SDS-PAGE and blotted onto a PVDF membrane (Millipore). To minimize background staining due to non-specific membrane-binding of the antibody, the membranes were directly blocked with a blocking buffer (5% (w/v) non-fat dry milk powder, 2% (w/v) bovine serum albumin, in Tris-buffered saline with 0.15% Tween-20 (TBST) for 1 hour at room temperature. Then they were probed with the primary antibodies anti-hACE2 mouse monoclonal antibody, clone AC18Z (1:1000, Millipore), or anti-β-actin mouse monoclonal antibody, clone C4 (1:2000, Sigma Aldrich) at 4°C overnight. After washing with TBST (10 minutes, three times), the membranes were incubated with a peroxidase-conjugated anti-mouse IgG secondary antibody (1:20.000, GE Healthcare, Milan, Italy) for 1 hour at room temperature. Chemioluminescence was detected by Clarity Max Western ECL Substrate Hybridization (Bio-Rad), and the membranes were scanned with a ChemiDoc XRS Touch Imaging System (Bio-Rad).

*Statistical Analysis*

Statistical analyses were performed using Prism GraphPad software v.10.2 (GraphPad Software, San Diego, CA, USA). All data points were included, except for experiments where negative and/or positive controls did not give the expected outcome. The analysis of outliers was performed. Data were analyzed using an unpaired *t*-test, one-way or two-way ANOVA corrected by a Bonferroni *post hoc* test, and the results were expressed as means ± SD or ± SEM. A *p*-value less than 0.05 was

 doi:10.20944/preprints202509.1598.v1



considered significant. For lifespan and health span studies, the number of dead and censored animals was used for survival analysis in OASIS 2 [19]. The *p*-values were calculated using the log-rank and Bonferroni's *post hoc* test between the pooled populations of animals.

## 3. Results

### *3.1. The Expression of hACE2 in C. elegans Affects the Reproduction and the Pharyngeal Function*

The new C. elegans strain expressing hACE2::mCherry under the vha-6 promoter (**Figure 1A**) was characterized. The level of hACE2 protein expression was assessed by Western blot analysis of lysates from WT and ACE2 worms on the first day of adulthood. Immunoreactive bands at approximately 135 kDa and 270 kDa, representing monomeric and dimeric forms of ACE2::mCherry, respectively, were detected in lysates of ACE2 worms but not in WT ones (**Figure 1B**). Some immunoreactive signals were also observed at a molecular weight lower than 135 kDa. Similar, though less intense, bands appeared in lysates of WT worms and were absent in recombinant hACE2 protein (**Figure 1B**). Based on these results, we concluded that the immunoreactive signals below 135 kDa likely result from the antibody against hACE2 binding to C. elegans proteins similar to the human ACE2 ortholog.

The impact of hACE2 expression on worm reproduction, development, feeding behavior, neuromuscular movement, lifespan, and health span was evaluated. A 22% reduction in the broad size, measured as the total number of progeny, was observed in ACE2 compared to WT (**Figure 1C**), indicating that the hACE2 expression affected the worm's reproduction. No effect was observed on the worms' development, as indicated by the number of worms at different larval stages (from L3 up to the adult stage), which was similar between ACE2 and WT nematodes (**Figure S1)**. The neuromuscular function and the feeding behavior of adult worms were then evaluated by scoring the number of left-right movements in liquid per minute (body bends/minute) and the function of the pharynx. No difference was observed between the movements of WT and ACE2 nematodes (**Figure 1D**), whereas there was a slight, but significant 5% reduction in the pharyngeal pumping rate of ACE2 (**Figure 1E**). The ability of worms to react to oxidative stress was similar between the two strains, as demonstrated by the comparable reduction in the pharyngeal pumping scored for WT and ACE2 nematodes after exposure to hydrogen peroxide (**Figure 1F**). Furthermore, the transgenic strain's lifespan and health span were similar between the two strains (**Figure S2)**. In particular, the median lifespan was 20.3 ± 0.40 days and 19.9 ± 0.37 days for WT and ACE2 nematodes, respectively, and the median health span was 18.0 ± 0.32 days and 18.6 ± 0.37 days for WT and ACE2, respectively. These findings indicate that the expression of the hACE2 receptor in nematodes reduced their ability to reproduce and the pharyngeal function.

 doi:10.20944/preprints202509.1598.v1



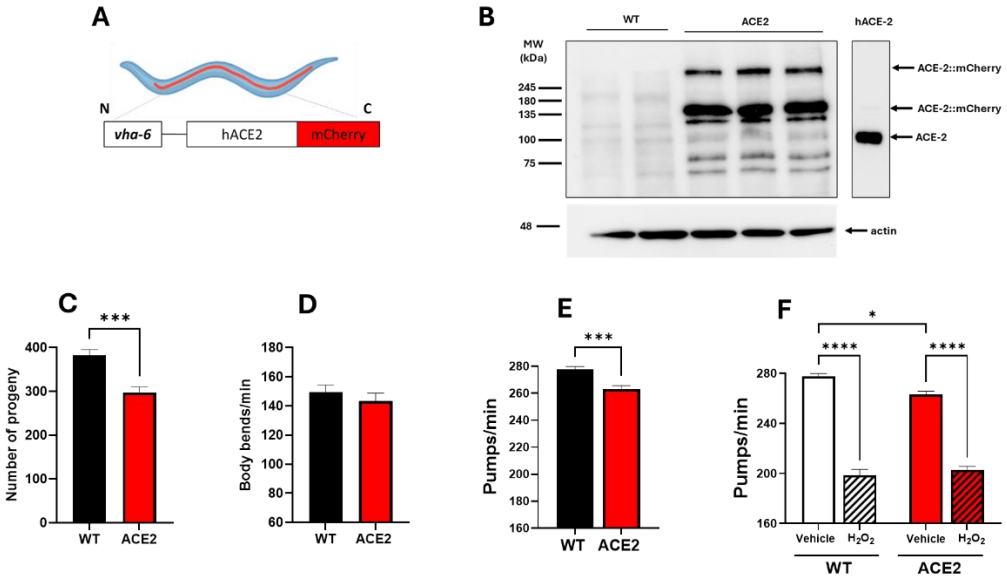


**Figure 1. Characterization of the transgenic C. elegans ACE2 strain. (A)** Schematic representation of the ACE2 transgenic C. elegans characterized in this study. The human ACE2::mCherry protein was mainly expressed in intestinal cells under the vha-6 promoter to generate an ACE2 transgenic C. elegans. (**B**) Western blots of transgenic ACE2 (ACE2) and wild-type (WT) worms (N=3 biological replicates). An equal amount of proteins (25 μg) was loaded in each gel lane and immunoblotted with anti-human ACE2 or anti-actin antibodies. Twenty ng of recombinant human ACE2 (hACE-2) were analyzed as a positive control. (**C**) Broad size of WT and ACE2 worms. Data are the mean ± SEM (N=7). *** p=0.0003, Student's t-test. (**D**) Motility and (**E**) pharyngeal activity of worms on the first day of adulthood. Data are expressed as the mean of (**D**) body bends/min (N = 10 worms/assay, 2 assays) or (**E**) pumps/min ± SEM (N = 12 worms/assay, 3 assays, **p = 0.0001, Student's t-test). (**F**) Sensitivity of worms to hydrogen peroxide. Worms were fed for 2 h with 0.5 mM $H_2O_2$ in 10 mM PBS, pH 7.4, or the same volume of PBS alone (Vehicle). Pharyngeal pumping was scored 24 hours after plating nematodes on NGM agar plates seeded with E. Coli OP50. Data are the mean of pumps/min ± SEM (N = 13 worms/assay, 4 assays). *p<0.05 and ****p<0.0001; interaction WT/$H_2O_2$ and ACE2/$H_2O_2$ p<0.005, two-way ANOVA, and Bonferroni's post hoc test.

*3.2. RBD Administration to ACE2 Worms Causes a Specific Pharyngeal Dysfunction*

To mimic the infection with SARS-CoV-2, ACE2 worms were fed with the RBD of SARS-CoV-2 in the Wuhan variant, and the onset of a toxic effect was determined by evaluating the worms' pharyngeal motility and locomotion 2 and 24 hours after the administration [11]. As shown in **Figure 2A and B**, RBD caused a dose-dependent pharyngeal impairment in ACE2 but not in WT worms. The pumping rate of ACE2 scored 2 hours after the RBD administration was significantly reduced, starting from the concentration of 0.1 ng/mL and reaching the minimum value at 10 ng/mL (**Figure 2A**). At this time point, the half-maximal inhibitory concentration (IC50) value of RBD was 0.96 ng/mL ± 1.39. A thirty-three times lower IC50 value of 0.029 ng/mL ± 1.21 was measured 24 hours after the RBD administration (**Figure 2B**), indicating that it caused a worsening and permanent pharyngeal dysfunction. At 100 ng/mL, RBD caused a 30.0% and 25.5% inhibition of the pharyngeal pumping in ACE2 worms 2 and 24 hours after the administration (**Figure 2C-D**). At this concentration, RBD did not affect the motility of ACE2 worms (**Figure S3**). Based on these results, the RBD concentration of 100 ng/mL was chosen for future experiments.

 doi:10.20944/preprints202509.1598.v1



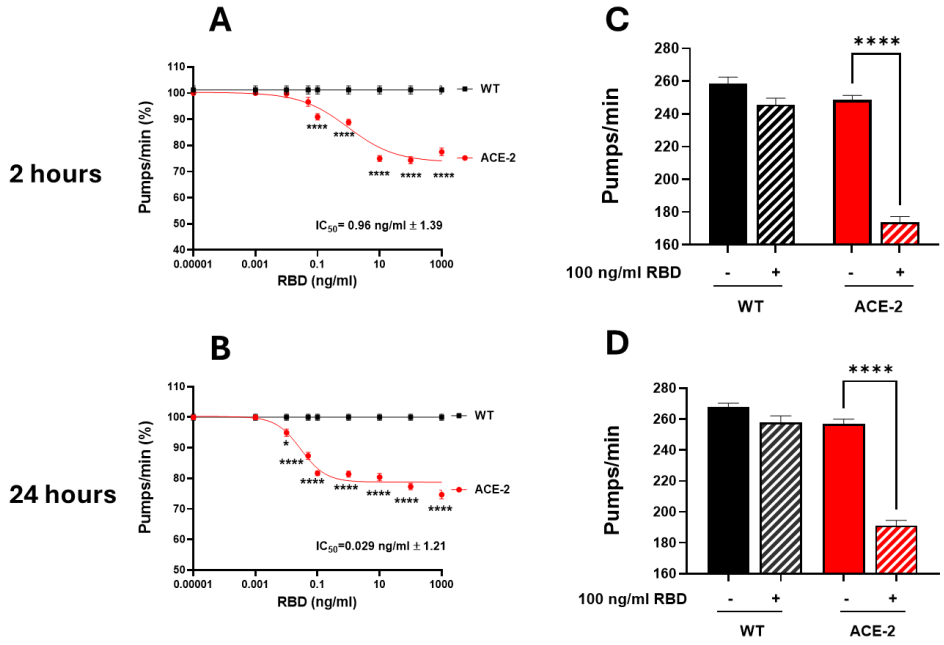


**Figure 2. RBD administration caused a specific toxic effect in ACE2 transgenic worms**. (**A, B**) Dose-dependent effect of RBD on the pharyngeal behavior of WT and ACE2 worms. Worms were fed for 2 hours with increasing concentrations of RBD suspended in 10 mM PBS or the same volume of PBS alone as a control. Pharyngeal pumping was scored (**A**) 2 and (**B**) 24 hours after plating nematodes on NGM agar plates seeded with E. coli OP50. Data are expressed as pumps/min (percentage of control) ± SEM (N = 10 worms/assay, 3 assays). *p<0.05 and ****p<0.0001 vs. WT treated with the corresponding concentration of RBD, one-way ANOVA, and Bonferroni's post hoc test. (**C, D**) Effect of 100 ng/mL RBD on the pharyngeal activity of WT and ACE2 worms scored (**C**) 2 and (**D**) 24 hours after the administration. Data are the mean of pumps/min ± SEM (N = 24 worms). ****p<0.0001; interaction RBD/ACE2 worms = p<0.0001, two-way ANOVA, and Bonferroni's post hoc test.

To determine if the toxic effect of the RBD administration was specifically due to the interaction of RBD with the hACE2 receptors expressed in the transgenic nematodes, ACE2 worms were administered with 100 ng/mL RBD in the presence or absence of the anti-hACE2, and the pharyngeal pumping rate was scored 2 and 24 hours later. Control worms were treated with 10 mM PBS, pH 7.4 (Vehicle) or the anti-hACE2 diluted in vehicle (**Figure 3A**). The anti-hACE2 previously inactivated by incubation at 100°C for 15 minutes was also administered as an additional control (**Figure 3A**). The anti-hACE2 alone did not affect the worms' pharynx (**Figure 3B-C**), but when co-administered with RBD, it completely abolished the RBD-induced pharyngeal toxicity (**Figure 3B-C**). These findings indicate that RBD causes a specific and permanent pharyngeal dysfunction in ACE2 nematodes mediated by the interaction with the ACE2 receptor. In addition, the pharyngeal dysfunction caused by RBD can be used to read out the mimicked infection.

 doi:10.20944/preprints202509.1598.v1



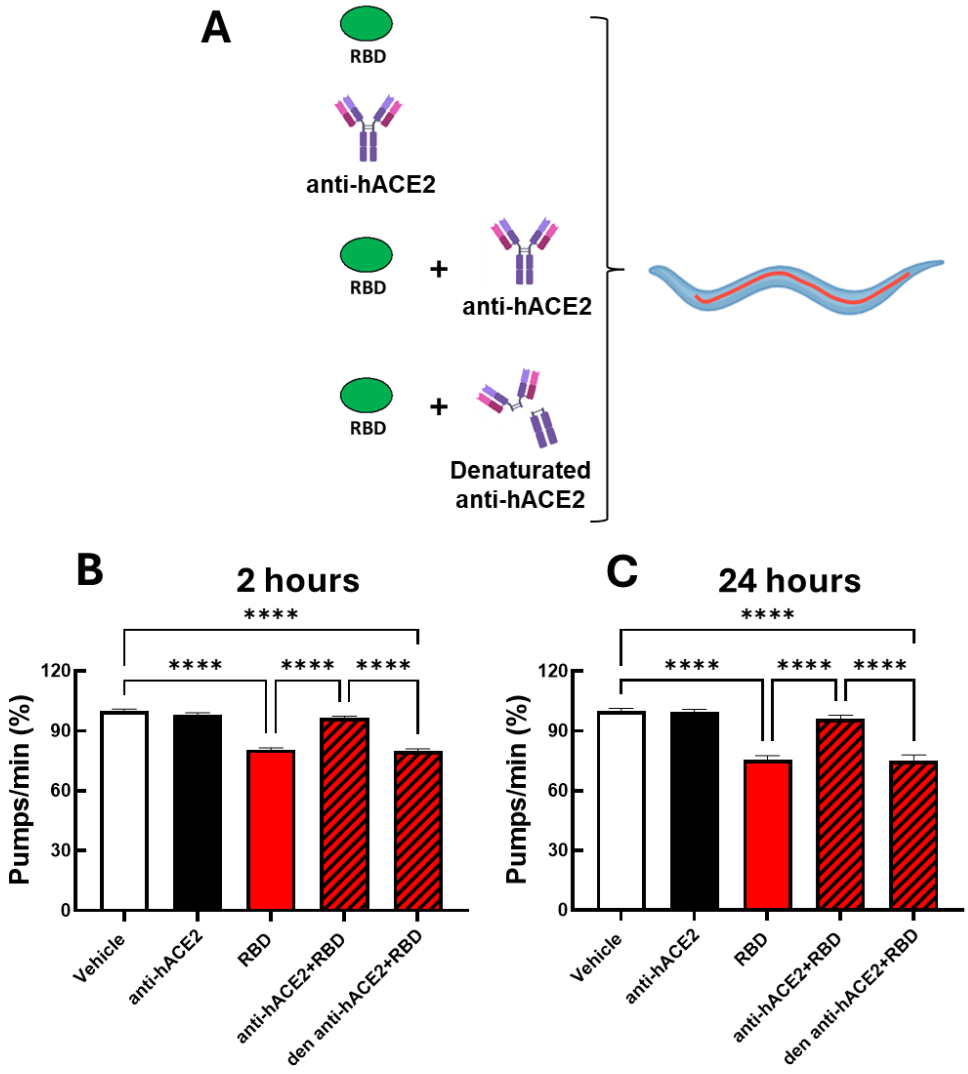


**Figure 3. Anti-hACE2 antibody counteracted the RBD toxic effect in ACE2 worms**. (**A**) Schematic representation of the treatment of worms with 100 ng/mL RBD alone or with the mouse monoclonal anti-human ACE2 antibody (anti-hACE2) (1:200 (vol/vol) RBD: anti-hACE2). The anti-hACE2 alone or 100 ng/mL RBD, administered with the inactivated anti-hACE2 (Denaturated anti-hACE2), were administered as negative controls. (**B, C**) ACE2 worms were fed for 2 hours with 100 ng/mL RBD in 10 mM PBS, pH 7.4, (RBD), 10 mM PBS, pH 7.4, alone (Vehicle), anti-hACE2 antibody diluted in 10 mM PBS, pH 7.4 (1:200, vol/vol), 100 ng/mL RBD + anti-ACE2 antibody (anti-hACE2 + RBD), or 100 ng/mL RBD + denatured antihACE2 antibody (den anti-hACE2 + RBD). Pharyngeal pumping was scored (**B**) 2 and (**C**) 24 hours after plating nematodes on NGM agar plates seeded with E. coli OP50. Data are the mean of pumps/min (% of vehicle-treated worms) ± SEM (N = 40 worms/assay, 4 assays). ****p<0.0001; interaction RBD/anti-hACE2 p<0.0001 at 2 and 24 h, according to two-way ANOVA, and Bonferroni's post hoc test.

*3.3. Raloxifene Reduces the Entry of Lentiviral Particles Expressing SARS-CoV-2 Spike Variants In Vitro*

Before using ACE2 worms for pharmacological studies with Raloxifene, we assessed the drug's ability to reduce viral entry in vitro. We used HEK293-ACE2 cells and first evaluated the potential cytotoxic effects of Raloxifene to select drug concentrations that did not impair cell viability. After 24 hours of exposure, Raloxifene significantly decreased the viability of HEK293-ACE2 cells starting at 10 μM, with maximal toxicity observed at 30 μM (**Figure 4**). Based on these findings, we chose Raloxifene concentrations of 1 and 3 μM for subsequent transduction experiments, where cells were infected with pseudotyped lentiviral vectors carrying different fluorochromes as reporter genes.

 doi:10.20944/preprints202509.1598.v1



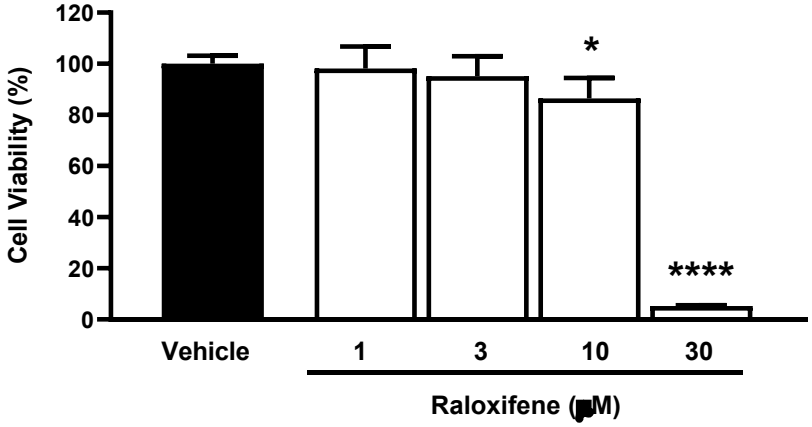


**Figure 4. Effect of Raloxifene on cell viability**. HEK293-ACE2 cells were treated with increasing concentrations of Raloxifene previously dissolved at 10 mM in DMSO and diluted in DMEM. Control cells were treated with an equivalent DMSO concentration (Vehicle). The cell viability was evaluated 24 hours after treatment using the MTT assay. Data are the mean ± SD of the percentage of viable cells compared to vehicle-treated cells. *$p$<0.05 and ****$p$ <0.0001 vs. Vehicle according to one-way ANOVA and Bonferroni's *post hoc* test.

HEK293-ACE2 cells were treated with Raloxifene previously dissolved at 10 mM in DMSO and diluted in DMEM, and then infected with lentivirus expressing the Spike protein of SARS-CoV-2 in Wuhan, B.1.1.7 UK, B.1.351 SA, or B.1.1.529 Omicron variant. Control cells were transduced with an equivalent DMSO concentration (Vehicle). In addition, HEK293 cells were infected with pseudoviral particles exposing SARS-CoV-2 Wuhan or B.1.351 SA as additional negative controls. As already reported by our group, no transduction was observed in HEK293 cells not expressing hACE2 (data not shown) [18]. Vehicle-treated HEK293-ACE2 cells were efficiently infected with all the different lentiviral variants tested (**Figure 5A)**. The lowest transduction capability was observed in cells pseudo-infected with the Wuhan variant, and the highest transduction was detected with B.1.1.529 Omicron one (**Figure 5A**). Raloxifene significantly inhibited the transduction of HEK293-ACE2 cells in a concentration-dependent manner with all the variants (**Figure 5A-B)**. One μM Raloxifene reduced the percentage of transduction by 15%, 40% and 36% in cells infected with the Wuhan variant, B.1.1.7 UK, and B.1.1.529 Omicron isoforms, respectively (**Figure 5B**). In contrast, no effect was observed in cells treated with lentivirus expressing B.1.351 SA Spike (**Figure 5B**). At 3 μM, Raloxifene reduced the percentage of transduced cells by 79%, 85% and 73% in cells infected with the Wuhan, B.1.1.7 UK, and B.1.1.529 Omicron variants, respectively. In contrast, a significantly lower protective effect was observed in cells infected with the B.1.351 SA variant, in which the percentage of transduced cells was reduced by 43% (**Figure 5B**). These results indicate that Raloxifene can act on the viral pre-entry phase of the infection, counteracting the infection.

Additional experiments were performed using lentiviral particles exposing Spike carrying the RBD-mutated N501Y or the P681H single-point mutation present within the furin cleavage site region of the spike protein. We observed a higher transduction capability in cells pseudo-infected with the N501Y variant, compared with the P681H variant (**Figure 5C**). Raloxifene significantly inhibited the entry of pseudovirus carrying the N501Y mutation by 57% only at 3 μM (**Figure 5C-D**); to a lower extent compared to its ability to inhibit the entry of the Wuhan variant (**Figure 5B, D**). These data suggest that the N501Y mutation in RBD, known to determine a tight interaction between RBD and the hACE receptor [20], is relevant for the Raloxifene effect confirming that its protection mechanism involves the interaction with hACE2. In cells transduced with lentivirus carrying the P681H spike substitution, Raloxifene was effective at 1 and 3 μM (**Figure 5C-D**), indicating that the presence of this mutation on the spike glycoprotein did not affect the drug's protective activity. All together, these data firmly supported the capacity of Raloxifene to reduce the pseudovirus entry in vitro.

 doi:10.20944/preprints202509.1598.v1



To exclude that this biological outcome could be ascribed to an effect of Raloxifene on hACE2 expression, even in cells modified to overexpress the protein constitutively, Western blot analysis was performed on lysates of HEK293-ACE2 cells treated for 3 up to 24 hours with the drug at 3 µM. Raloxifene did not modify the expression of the hACE2 (**Figure S4**), indicating that its ability to reduce the entry of SARS-CoV-2 pseudovirus in vitro is not mediated by the modulation of this host cell receptor expression.

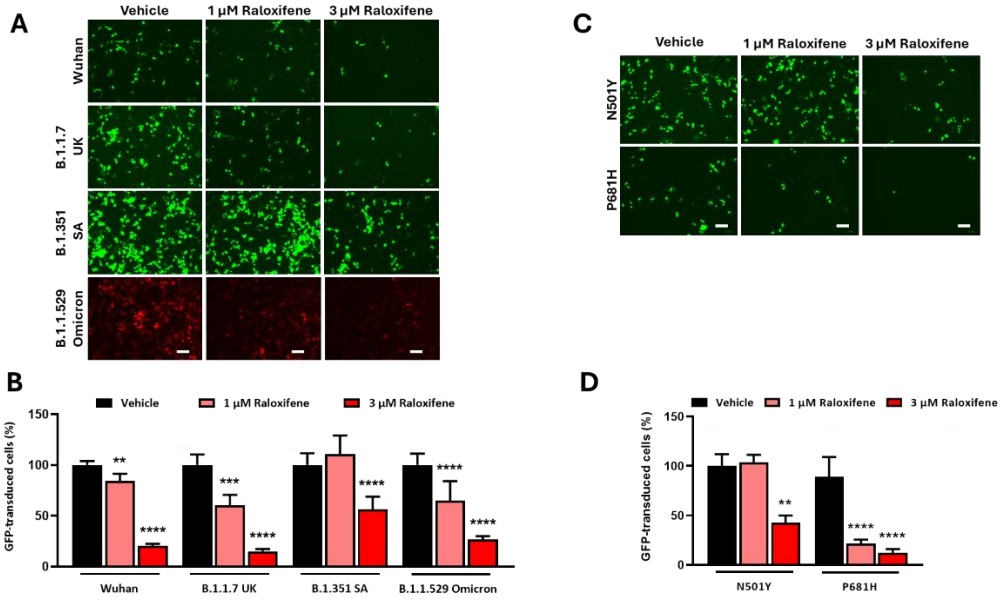


**Figure 5. Raloxifene reduced pseudoviral transduction in vitro.** (**A, B**) HEK293-ACE2 were pre-incubated for 4 hours with 1 µM or 3 µM Raloxifene previously dissolved at 10 mM in DMSO and diluted in DMEM. Control cells were treated with an equivalent DMSO concentration (Vehicle). Cells were then infected with pseudoviral particles exposing SARS-CoV-2 Wuhan, B.1.1.7 UK, B.1.351 SA, or B.1.1.529 Omicron Spike variant. **(A)** Representative fluorescence microscopy images obtained. Scale bar, 100 µm. (**B**) GFP- and RFP-transduced HEK293-ACE2 cells expressed as a percentage of Vehicle-treated cells. Data are the mean ± SD (N=4-10, 3 independent experiments). ***p*<0.001, ****p*< 0.0005, and **** *p*< 0,0001 vs. the corresponding Vehicle according to one-way ANOVA and Bonferroni's *post hoc* test. **(C, D)** HEK293-ACE2 cells were pre-incubated for 4 hours with 1 µM or 3 µM Raloxifene previously dissolved at 10 mM in DMSO and diluted in DMEM. Control cells were treated with an equivalent DMSO concentration (Vehicle). Cells were then infected with pseudoviral particles exposing the RBD-mutated N501Y or P681H-mutated spike variant. **(C)** Representative fluorescence microscopy images. Scale bar, 100 µm. (**D**) GFP-transduced HEK293-ACE2 cells expressed as a percentage of Vehicle-treated cells. Data are the mean ± SD (N=3-10, 3 independent experiments). ***p*<0.001, and **** *p*< 0,0001 vs. the corresponding Vehicle according to one-way ANOVA and Bonferroni's *post hoc* test.

### *3.4. Raloxifene Protects ACE2 Transgenic Worms from the Toxic Effect of RBD*

Transgenic C. elegans expressing ACE2 treated with RBD was employed as a model to evaluate the protective effect of Raloxifene in vivo. First, the possible toxic effect of Raloxifene was considered by administering transgenic worms with increasing drug concentrations (0.1-5 µM). As shown in **Figure 6A**, Raloxifene did not affect the physiological pharyngeal function of worms at any of the doses considered.

Raloxifene was then administered to worms exposed to 100 ng/mL RBD, and the pharyngeal function was scored 24 hours later. Significant protection from the toxicity caused by RBD was observed starting from 0.01 µM Raloxifene, and a complete counteraction of the pharynx dysfunction was reached at 0.1 µM (**Figure 6B**). At this concentration, Raloxifene, already after 2 hours of administration, restored the defect in pharyngeal contraction induced by RBD, bringing the organ

 doi:10.20944/preprints202509.1598.v1



function back to the physiological level (**Figure 6C**). Interestingly, the effect of Raloxifene persisted with time since its beneficial effect was still present 24 hours after the administration (**Figure 6D**). This protective effect could be ascribed to the ability of Raloxifene to bind to RBD, thus counteracting its interaction with hACE2 receptors.

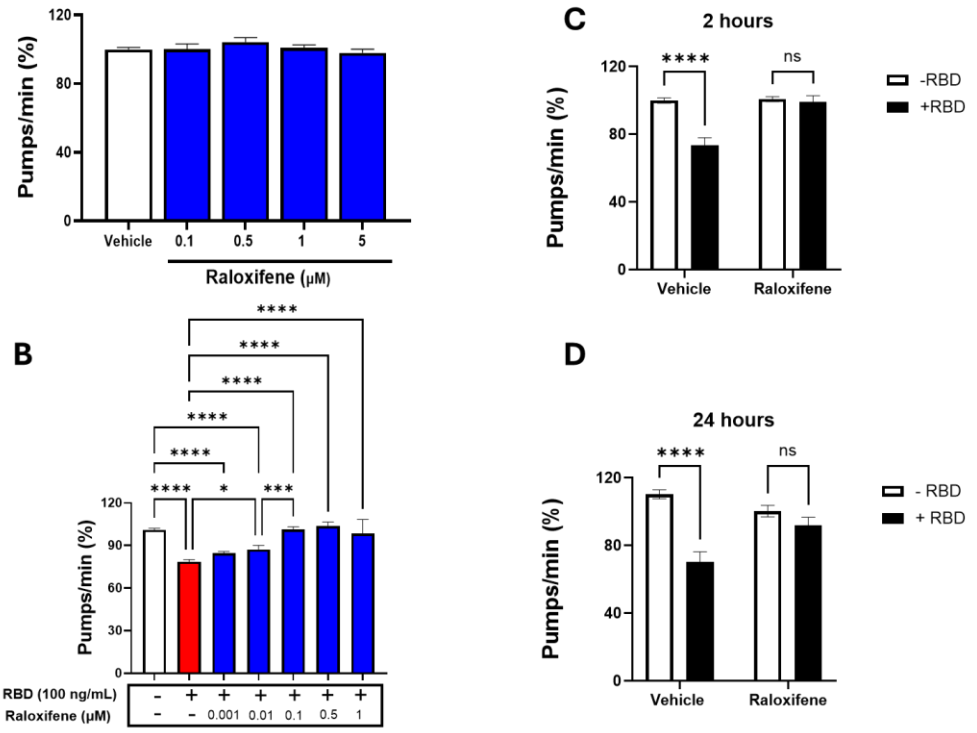


**Figure 6. Raloxifene protected ACE2 worms from the toxicity induced by RBD. (A-B)** ACE2 worms were fed for 2 h with **(A)** Raloxifene dissolved in DMSO at 10 mM and diluted to 0.1- 5 µM in 10 mM PBS, pH 7.4, or with **(B)** 100 ng/ml RBD alone or together with different concentrations of Raloxifene. Control worms were fed the same volume of DMSO diluted in 10 mM PBS, pH 7.4 (Vehicle, white bar). Pharyngeal pumping was scored 24 hours after plating nematodes on NGM agar plates seeded with *E. coli OP50.* Data are expressed as pumps/min (percentage of Vehicle-treated worms) ± SEM (N = 20). **p*< 0.05, ****p*<0.001, *****p*<0.0001, one-way ANOVA, and Bonferroni's *post hoc* test. **(C, D)** ACE2 worms were fed for 2 h with Raloxifene dissolved in DMSO at 10 mM and diluted to 1 µM in 10 mM PBS, pH 7.4,(Raloxifene) or DMSO diluted in 10 mM PBS, pH 7.4 (Vehicle) in the presence (+RBD) or absence (-RBD) of 100 ng/mL RBD. Pharyngeal pumping was scored **(C)** 2 and **(D)** 24 hours after plating nematodes on NGM agar plates seeded with *E. Coli* OP50. Data are expressed as pumps/min (percentage of Vehicle-treated worms) ± SEM. *****p*<0.0001; interaction RBD/Raloxifene *p*= 0.0003 and 0.0014 at 2 and 24 hours, respectively, according to two-way ANOVA and Bonferroni's *post hoc* test.

## 4. Discussion

The nematode C. elegans is widely used to study the mechanisms behind various human diseases [21,22] and is an emerging model for exploring host-pathogen interactions. In nature, this worm lives in a microbially rich environment where it encounters different types of pathogenic microorganisms, including bacterial, viral, fungal, and oomycete pathogens [21,22]. C. elegans has already been used as a model host and a tool for studying the biology of various human bacterial infections and fungal pathogens, as well as discovering new antimicrobial treatments [23–27].

In this study, we propose using a new transgenic C. elegans strain constitutively expressing the hACE2 treated with the RBD to mimic the SARS-CoV-2 infection. Being hACE2 expressed under the vha6 promoter, it was almost ubiquitously present in all the worm's organs, including the pharynx and intestine, the primary food access routes. We reported for the first time that the expression of hACE2 significantly impaired the reproductive capacity of worms as well as their feeding behavior.

 doi:10.20944/preprints202509.1598.v1



When these worms were treated with RBD, we observed a specific, dose-dependent, and permanent pharyngeal dysfunction, suggesting that interaction with hACE2 can activate unusual mechanisms that sustain organ damage over time. The data from experiments using an anti-hACE2 antibody also demonstrated the link between pharyngeal dysfunction and the RBD/hACE2 interaction. Additionally, C. elegans avoided the orthologue of transmembrane serine protease 2, a protease essential for the entry pathway of SARS-CoV-2 [28], ruling out the possibility that the toxic effect of RBD is due to the activation of some intracellular proteolytic cleavages.

Although *C. elegans* is provided only by innate immunity and lacks many aspects of the vertebrate innate immune system, like cellular immunity, inflammasome, and complement, it can recognize viral replication products. Notably, this is the first evidence that, besides viral nucleic acids [29], a viral protein can induce the onset of specific defense mechanisms in *C. elegans*, like inhibiting the feeding behavior. In addition, viral and fungal pathogens can activate an immunological intracellular response to pathogens resembling the vertebrate-specific type-I interferon response [29]. Thus, the transgenic *C. elegans* strain expressing the hACE2 might represent a good model for rapidly investigating the effect of new coronavirus variants using hACE2 as a cell entry receptor. This nematode expresses ADM-4, an ortholog of human ADAM-17, that is upregulated by SARS-CoV-2, facilitating its entry into cells [30]. It has recently been reported that the infection of worms with *Klebsiella aerogenes* caused a significant upregulation of *adm-4* and the reduction of pharyngeal pumping [31]. Thus, it cannot be excluded that RBD administration to ACE2 worms could also affect *adm-4* expression and activate some signaling pathways relevant to the innate immunity regulation of *C. elegans*. Because of its ability to be genetically manipulated, *C. elegans* could represent a robust system for studying the defense mechanisms of non-professional immune cells in a whole-animal context.

Raloxifene was selected as a prototype drug for investigating the potential use of the ACE2 C. elegans strain for pharmacological studies. It was first tested on HEK293-ACE2 cells, a relevant experimental system for investigating the role of hACE2 as the cell entry receptor, before being used to validate the use of ACE2 worms for pharmacological purposes. Although this drug was selected in the EXSCALATE platform for its ability to bind relevant SARS-CoV-2 proteins, the data obtained from surface plasmon resonance experiments indicated that it did not interfere with ACE2-Spike subunit 1 binding. The data obtained in HEK293-ACE2 cells indicated that administering Raloxifene before adding pseudovirus can inhibit the infection. Interestingly, Raloxifene inhibited the entry of lentivirus expressing the spike protein of different SARS-CoV-2 variants at 1-3 μM, concentrations similar to those reported to inhibit viral replication in vitro [15]. These findings suggested that this drug can act in vitro on processes that could be involved in Spike-hACE2 interaction.

Raloxifene also effectively protected ACE2 worms from the toxicity caused by RBD administration. This is the first observation of this drug's ability to interfere with the RBD engagement of hACE2 in vivo. Raloxifene has been reported to have pleiotropic effects involving multiple mechanisms and processes, including the downregulation of ADAM17 [30]. Additional studies are required to investigate whether Raloxifene can modulate the expression of adm-4 in ACE2 worms and if this effect could be linked to its protective effect.

Altogether, these findings indicate that the transgenic C. elegans strain expressing hACE2 can represent an affordable approach for screening in vivo the effects of molecules mediated by the interaction with the hACE2 receptor. In addition, generating genetically modified C. elegans to express proteins relevant to vertebrate infection could help model the interaction with pathogens and validate the protective effect of molecules with antiviral activity quickly and cheaply.

**Supplementary Materials:** The following supporting information can be downloaded at the website of this paper posted on Preprints.org. Figure S1: Human ACE2 expression in *C. elegans* did not affect the development; Figure S2: Human ACE2 expression in *C. elegans* did not affect the life span and health span; Figure S3: RBD administration did not modify the motility of worms; Figure S4: Raloxifene did not affect the expression of ACE2 in HEK293-ACE2 cells.

 doi:10.20944/preprints202509.1598.v1



**Author Contributions:** The following statements should be used: "Conceptualization, L.D. and M.R.; methodology, M.R., S.B., M.M.B., A.D.L.; formal analysis, M.R., S.B., M.M.B.; investigation, M.R., S.B., M.M.B., S.G.; writing—original draft preparation, M.R., S.B., L.D.; writing—review and editing, M.R., S.B., L.D., M.F., D.I., A.R.B.; funding acquisition, L.D., A.R.B. All authors have read and agreed to the published version of the manuscript.

**Funding:** This research was supported by EU funding within the NextGenerationEU-MUR PNRR Extended Partnership initiative on Emerging Infectious Diseases (Project no. PE00000007, INF-ACT) (L.D. and M.R.) and by Horizon 2020 European Project "N.101003551-EXSCALATE4CoV" (D.I. and A.R.B.).

**Data Availability Statement:** The article and its Supplementary Information contain all relevant data. All raw data have been deposited to zenodo.org and can be requested at luisa.diomede@marionegri.it.

**Acknowledgments:** OP50 Escherichia coli bacteria were provided by the Caenorhabditis Genetics Center (CGC), which is funded by the National Institutes of Health (NIH) Office of Research Infrastructure Programs (P40 OD010440).

**Conflicts of Interest:** D.I. and A.R.B. are employees of EXSCALATE, Dompé Farmaceutici SpA. The other authors declare no conflicts of interest.

## Abbreviations

The following abbreviations are used in this manuscript:

| | |
|---|---|
| COVID-19 | Coronavirus Disease 2019 |
| *C. elegans* | *Caenorhabditis elegans* |
| hACE2 | Human angiotensin-converting enzyme 2 |
| RBD | Receptor-Binding Domain |
| WT | wild-type Nematodes |
| HEK293-ACE2 | human embryonic kidney 293-T cells stably expressing hACE2 |
| ACE2 | transgenic *C. elegans* strain expressing the human ACE2 |
| vha6 | Vacuolar H ATPase-6 |
| PBS | phosphate-buffered saline |
| *E. coli* | Escherichia coli |
| NGM | Nematode Growth Media |
| DMEM | Dulbecco Modified Eagle Medium |
| FBS | fetal bovine serum |
| DMSO | dimethyl sulfoxide |
| MTT | 3-(4,5-dimethylthiazol-2-yl)-2,5 2,5-diphenyltetrazolium bromide |
| anti-hACE2 | anti-hACE2 mouse monoclonal antibody |

## References

1. COVID-19 Deaths | WHO COVID-19 Dashboard Available online: https://data.who.int/dashboards/covid19/cases (accessed on 8 September 2025).
2. Zhao, Y.; Wang, C.-L.; Gao, Z.-Y.; Qiao, H.-X.; Wang, W.-J.; Liu, X.-Y.; Chuai, X. Ferrets: A Powerful Model of SARS-CoV-2. *Zool Res* **2023**, *44*, 323–330, doi:10.24272/j.issn.2095-8137.2022.351.
3. Gammon, D.B. Caenorhabditis Elegans as an Emerging Model for Virus-Host Interactions. *J Virol* **2017**, *91*, e00509-17, doi:10.1128/JVI.00509-17.
4. Martineau, C.N.; Kirienko, N.V.; Pujol, N. Innate Immunity in C. Elegans. In *Current Topics in Developmental Biology*; Elsevier, 2021; Vol. 144, pp. 309–351 ISBN 978-0-12-816177-7.
5. Pradel, E.; Zhang, Y.; Pujol, N.; Matsuyama, T.; Bargmann, C.I.; Ewbank, J.J. Detection and Avoidance of a Natural Product from the Pathogenic Bacterium *Serratia Marcescens* by *Caenorhabditis Elegans*. *Proc. Natl. Acad. Sci. U.S.A.* **2007**, *104*, 2295–2300, doi:10.1073/pnas.0610281104.
6. Irazoqui, J.E.; Urbach, J.M.; Ausubel, F.M. Evolution of Host Innate Defence: Insights from Caenorhabditis Elegans and Primitive Invertebrates. *Nat Rev Immunol* **2010**, *10*, 47–58, doi:10.1038/nri2689.

 doi:10.20944/preprints202509.1598.v1




7. Brooks, D.R.; Appleford, P.J.; Murray, L.; Isaac, R.E. An Essential Role in Molting and Morphogenesis of Caenorhabditis Elegans for ACN-1, a Novel Member of the Angiotensin-Converting Enzyme Family That Lacks a Metallopeptidase Active Site. *Journal of Biological Chemistry* **2003**, *278*, 52340–52346, doi:10.1074/jbc.M308858200.
8. Frand, A.R.; Russel, S.; Ruvkun, G. Functional Genomic Analysis of C. Elegans Molting. *PLoS Biol* **2005**, *3*, e312, doi:10.1371/journal.pbio.0030312.
9. [Object Object] Available online: https://www.alliancegenome.org/gene/WB:WBGene00000039 (accessed on 8 September 2025).
10. Engelmann, I.; Pujol, N. Innate Immunity in C. Elegans. In *Invertebrate Immunity*; Söderhäll, K., Ed.; Advances in Experimental Medicine and Biology; Springer US: Boston, MA, 2010; Vol. 708, pp. 105–121 ISBN 978-1-4419-8058-8.
11. Natale, C.; Barzago, M.M.; Diomede, L. Caenorhabditis Elegans Models to Investigate the Mechanisms Underlying Tau Toxicity in Tauopathies. *Brain Sciences* **2020**, *10*, 838, doi:10.3390/brainsci10110838.
12. Hong, S.; Chang, J.; Jeong, K.; Lee, W. Raloxifene as a Treatment Option for Viral Infections. *J Microbiol.* **2021**, *59*, 124–131, doi:10.1007/s12275-021-0617-7.
13. Allegretti, M.; Cesta, M.C.; Zippoli, M.; Beccari, A.; Talarico, C.; Mantelli, F.; Bucci, E.M.; Scorzolini, L.; Nicastri, E. Repurposing the Estrogen Receptor Modulator Raloxifene to Treat SARS-CoV-2 Infection. *Cell Death Differ* **2022**, *29*, 156–166, doi:10.1038/s41418-021-00844-6.
14. Nicastri, E.; Marinangeli, F.; Pivetta, E.; Torri, E.; Reggiani, F.; Fiorentino, G.; Scorzolini, L.; Vettori, S.; Marsiglia, C.; Gavioli, E.M.; et al. A Phase 2 Randomized, Double-Blinded, Placebo-Controlled, Multicenter Trial Evaluating the Efficacy and Safety of Raloxifene for Patients with Mild to Moderate COVID-19. *eClinicalMedicine* **2022**, *48*, 101450, doi:10.1016/j.eclinm.2022.101450.
15. Iaconis, D.; Bordi, L.; Matusali, G.; Talarico, C.; Manelfi, C.; Cesta, M.C.; Zippoli, M.; Caccuri, F.; Bugatti, A.; Zani, A.; et al. Characterization of Raloxifene as a Potential Pharmacological Agent against SARS-CoV-2 and Its Variants. *Cell Death Dis* **2022**, *13*, 498, doi:10.1038/s41419-022-04961-z.
16. Diomede, L.; Romeo, M.; Rognoni, P.; Beeg, M.; Foray, C.; Ghibaudi, E.; Palladini, G.; Cherny, R.A.; Verga, L.; Capello, G.L.; et al. Cardiac Light Chain Amyloidosis: The Role of Metal Ions in Oxidative Stress and Mitochondrial Damage. *Antioxid. Redox Signal.* **2017**, *27*, 567–582, doi:10.1089/ars.2016.6848.
17. Leiser, S.F.; Jafari, G.; Primitivo, M.; Sutphin, G.L.; Dong, J.; Leonard, A.; Fletcher, M.; Kaeberlein, M. Age-Associated Vulval Integrity Is an Important Marker of Nematode Healthspan. *AGE* **2016**, *38*, 419–431, doi:10.1007/s11357-016-9936-8.
18. Beeg, M.; Baroni, S.; Piotti, A.; Porta, A.; De Luigi, A.; Cagnotto, A.; Gobbi, M.; Diomede, L.; Salmona, M. A Comprehensive Technology Platform for the Rapid Discovery of Peptide Inhibitors against SARS-CoV-2 Pseudovirus Infection. *IJMS* **2023**, *24*, 12146, doi:10.3390/ijms241512146.
19. Han, S.K.; Lee, D.; Lee, H.; Kim, D.; Son, H.G.; Yang, J.-S.; Lee, S.-J.V.; Kim, S. OASIS 2: Online Application for Survival Analysis 2 with Features for the Analysis of Maximal Lifespan and Healthspan in Aging Research. *Oncotarget* **2016**, *7*, 56147–56152, doi:10.18632/oncotarget.11269.
20. Yi, C.; Sun, X.; Ye, J.; Ding, L.; Liu, M.; Yang, Z.; Lu, X.; Zhang, Y.; Ma, L.; Gu, W.; et al. Key Residues of the Receptor Binding Motif in the Spike Protein of SARS-CoV-2 That Interact with ACE2 and Neutralizing Antibodies. *Cell Mol Immunol* **2020**, *17*, 621–630, doi:10.1038/s41423-020-0458-z.
21. Apfeld, J.; Alper, S. What Can We Learn About Human Disease from the Nematode C. Elegans? In *Disease Gene Identification*; DiStefano, J.K., Ed.; Methods in Molecular Biology; Springer New York: New York, NY, 2018; Vol. 1706, pp. 53–75 ISBN 978-1-4939-7470-2.
22. Markaki, M.; Tavernarakis, N. Modeling Human Diseases in *Caenorhabditis Elegans*. *Biotechnology Journal* **2010**, *5*, 1261–1276, doi:10.1002/biot.201000183.
23. Vallejo, J.A.; Beceiro, A.; Rumbo-Feal, S.; Rodríguez-Palero, M.J.; Russo, T.A.; Bou, G. Optimisation of the Caenorhabditis Elegans Model for Studying the Pathogenesis of Opportunistic Acinetobacter Baumannii. *International Journal of Antimicrobial Agents* **2015**, S0924857915002411, doi:10.1016/j.ijantimicag.2015.05.021.
24. Ewbank, J.J.; Zugasti, O. *C. Elegans*: Model Host and Tool for Antimicrobial Drug Discovery. *Disease Models & Mechanisms* **2011**, *4*, 300–304, doi:10.1242/dmm.006684.

 doi:10.20944/preprints202509.1598.v1




25. Kim, W.; Hendricks, G.L.; Lee, K.; Mylonakis, E. An Update on the Use of *C. Elegans* for Preclinical Drug Discovery: Screening and Identifying Anti-Infective Drugs. *Expert Opinion on Drug Discovery* **2017**, *12*, 625–633, doi:10.1080/17460441.2017.1319358.
26. Jayamani, E.; Rajamuthiah, R.; Larkins-Ford, J.; Fuchs, B.B.; Conery, A.L.; Vilcinskas, A.; Ausubel, F.M.; Mylonakis, E. Insect-Derived Cecropins Display Activity against Acinetobacter Baumannii in a Whole-Animal High-Throughput Caenorhabditis Elegans Model. *Antimicrob Agents Chemother* **2015**, *59*, 1728–1737, doi:10.1128/AAC.04198-14.
27. Gill, M.S.; Olsen, A.; Sampayo, J.N.; Lithgow, G.J. An Automated High-Throughput Assay for Survival of the Nematode Caenorhabditis Elegans. *Free Radical Biology and Medicine* **2003**, *35*, 558–565, doi:10.1016/S0891-5849(03)00328-9.
28. Koch, J.; Uckeley, Z.M.; Doldan, P.; Stanifer, M.; Boulant, S.; Lozach, P. TMPRSS2 Expression Dictates the Entry Route Used by SARS-CoV-2 to Infect Host Cells. *The EMBO Journal* **2021**, *40*, e107821, doi:10.15252/embj.2021107821.
29. Lažetić, V.; Blanchard, M.J.; Bui, T.; Troemel, E.R. Multiple Pals Gene Modules Control a Balance between Immunity and Development in Caenorhabditis Elegans. *PLoS Pathog* **2023**, *19*, e1011120, doi:10.1371/journal.ppat.1011120.
30. Jocher, G.; Grass, V.; Tschirner, S.K.; Riepler, L.; Breimann, S.; Kaya, T.; Oelsner, M.; Hamad, M.S.; Hofmann, L.I.; Blobel, C.P.; et al. ADAM10 and ADAM17 Promote SARS-CoV-2 Cell Entry and Spike Protein-mediated Lung Cell Fusion. *EMBO Reports* **2022**, *23*, e54305, doi:10.15252/embr.202154305.
31. Gowripriya, T.; Meharaj Afrin, K.; Paurna, M.; Yashwanth, R.; Bhaskar, J.P.; Suresh, R.; Balamurugan, K. Regulation of miR-61 and Col-19 via TGF-β and Notch Signalling in Caenorhabditis Elegans against Klebsiella Aerogenes Infection. *Microbial Pathogenesis* **2024**, *186*, 106505, doi:10.1016/j.micpath.2023.106505.